

## Cep63 Recruits Cdk1 to the Centrosome: Implications for Regulation of Mitotic Entry, Centrosome Amplification, and Genome Maintenance

Harald Löffler<sup>1</sup>, Anne Fechter<sup>1</sup>, Marc Matuszewska<sup>1</sup>, Rainer Saffrich<sup>2</sup>, Martin Mistrik<sup>4</sup>, Joachim Marhold<sup>1</sup>, Christin Hornung<sup>1</sup>, Frank Westermann<sup>3</sup>, Jiri Bartek<sup>4,5</sup>, and Alwin Krämer<sup>1</sup>

### Abstract

Centrosomes are central regulators of mitosis that are often amplified in cancer cells. Centrosomes function both as organizers of the mitotic spindle and as reaction centers to trigger activation of Cdk1 and G<sub>2</sub>/M transition in the cell cycle, but their functional organization remains incomplete. Recent proteomic studies have identified novel components of the human centrosome including Cep63, a protein of unknown function that *Xenopus* studies have implicated in mitotic spindle assembly and spindle inactivation after DNA damage. Here, we report that human Cep63 binds to and recruits Cdk1 to centrosomes, and thereby regulates mitotic entry. RNAi-mediated Cep63 depletion in U2OS cancer cells induced polyploidization through mitotic skipping. Elicitation of this phenotype was associated with downregulation of centrosomal Cdk1, mimicking the phenotype induced by direct depletion of Cdk1. In contrast, Cep63 overexpression induced *de novo* centrosome amplification during cell-cycle interphase. Induction of this phenotype was suppressible by cell treatment with the Cdk inhibitor roscovitine. In a survey of 244 neuroblastoma cases, Cep63 mRNA overexpression was associated with *MYCN* oncogene amplification and poor prognosis. In cultured cells, Cep63 overexpression was associated with an enhancement in replication-induced DNA breakage. Together, our findings define human Cep63 as a centrosomal recruitment factor for Cdk1 that is essential for mitotic entry, providing a physical link between the centrosome and the cell-cycle machinery. *Cancer Res*; 71(6); 2129–39. ©2011 AACR.

### Introduction

Centrosomes function as microtubule-organizing centers and mitotic spindle poles, directing the formation of bipolar spindles (1, 2). To ensure spindle bipolarity, centrosomes normally duplicate precisely once per cell cycle, which occurs in parallel with DNA replication and is mediated by Cdk2 (1–6). Centrosome amplification has been frequently observed in

both solid and hematologic malignancies and has been linked to tumorigenesis (7). Both the preferred mechanism leading to and the relevant consequences of centrosome amplification are still controversial. Although Cdk2-dependent *de novo* synthesis of supernumerary centrosomes in interphase has been repeatedly postulated, centrosome amplification might alternatively result from polyploidization due to mitotic defects, or centrosomes might become fragmented (e.g., after DNA damage) rather than amplified (8–14). Moreover, a centrosome inactivation checkpoint has been postulated where amplification (or fragmentation) of centrosomes in response to DNA damage leads to elimination of damaged cells via mitotic catastrophe (8–12). On the other hand, in most cases, centrosome amplification does not induce widespread multipolar mitoses due to clustering of multiple centrosomes into a bipolar spindle array (15, 16). Rather, amplified centrosomes lead to low-level chromosomal instability caused by increased chromosome missegregation rates (17).

Centrosomes serve as reaction centers where key regulators meet to control cell-cycle transitions (8, 18). In particular, the G<sub>2</sub>/M transition is initiated by the activation of cyclin B1–Cdk1 at centrosomes, which is stimulated by Cdc25B and Aurora A but inhibited by centrosomal Chk1 (19–23). Similarly, cyclin E has been shown to localize to centrosomes, thereby promoting S-phase entry (24). Spatiotemporal orchestration of

**Authors' Affiliations:** <sup>1</sup>Clinical Cooperation Unit Molecular Hematology/Oncology, German Cancer Research Center and Department of Medicine V, University of Heidelberg; <sup>2</sup>Department of Medicine V, University of Heidelberg; <sup>3</sup>Department of Tumor Genetics, German Cancer Research Center, Heidelberg, Germany; <sup>4</sup>Laboratory of Genome Integrity and Institute of Molecular and Translational Medicine, Palacky University, Olomouc, Czech Republic; and <sup>5</sup>Institute of Cancer Biology and Centre for Genotoxic Stress Research, Danish Cancer Society, Copenhagen, Denmark

**Note:** Supplementary data for this article are available at Cancer Research online (<http://cancerres.aacrjournal.org/>).

H. Löffler and A. Fechter contributed equally to this work.

**Corresponding Author:** Alwin Krämer, Clinical Cooperation Unit Molecular Hematology/Oncology, German Cancer Research Center and Department of Medicine V, University of Heidelberg, Im Neuenheimer Feld 280, 69120 Heidelberg, Germany. Phone: 49-6221-42-1440; Fax: 49-6221-42-1444. E-mail: a.kraemer@dkfz.de

doi: 10.1158/0008-5472.CAN-10-2684

©2011 American Association for Cancer Research.

centrosome and DNA replication cycles with mitotic events are essential for both proper cell proliferation and maintenance of chromosomal integrity (1, 2, 8).

In a mass spectrometry-based proteomic screen for novel centrosomal components, Cep63 was among the most abundant newly identified proteins (25). In a study on *Xenopus* mitotic egg extracts, Cep63 was shown to be targeted by ATM- and ATR-dependent phosphorylation, leading to inactivation of centrosome-dependent spindle assembly in response to DNA double-strand breaks (DSB; ref. 26). Our present study documents the first functional analysis of Cep63 in mammalian cells. We describe a novel function of Cep63 in recruiting the key mitotic kinase Cdk1 to centrosomes and report on chromosomal instability and ploidy aberrations in human cells with disbalanced levels of Cep63, including cancer-associated overexpression that correlates with poor patient prognosis.

## Materials and Methods

### Plasmid construction

Transcript variant 3 of *Cep63* was provided by E.A. Nigg, variant 2 was purchased from ImaGenes (clone ID: IRALp962H1854Q2), other variants were produced by RT-PCR from BJ cells. All cDNAs were cloned into pEGFP-C1 (BD Biosciences Clontech). For stable transfection, pEGFP-*Cep63* (transcript variant 3) was cloned into a modified pcDNA4/TO (Invitrogen) vector whose selection cassette was changed from zeocin to puromycin.

### Cell culture, cell lines, and siRNAs

EBV-transformed lymphoblastoid cells (provided by L. Savelyeva), KE-37, and CCRF-CEM cells were cultured in RPMI 1640 (Gibco) and other cell lines were cultured in DMEM (PAA Laboratories Inc.), each supplemented with 10% fetal calf serum (Biocrom) and antibiotics. Cell line contaminations were excluded according to published methodology (27). Peripheral blood mononuclear cells of a healthy donor and a patient with chronic lymphocytic leukemia (CLL) were obtained by gradient centrifugation (Biocoll, 1.077 g/mL; Biocrom). Transfections were done using Oligofectamine (Invitrogen), Dharmafect (Thermo Scientific), or Fugene 6 (Roche). T-Rex-U2OS cells (Invitrogen) stably expressing GFP-Cep63 inducible by 1  $\mu$ g/mL tetracycline was generated using a modified T-Rex system (Invitrogen). The following siRNAs were used: 5'-GGCUCUGGUGAACAUCAdTdT-3', targeting exon 6 of *Cep63*, 5'-gaacuucgucauccaaauadTdT-3', targeting *Cdk1*, and 5'-UAAGGCUAUGAA GAGAUACdTdT-3', targeting *luciferase*.

### Antibodies

A GST-fusion peptide corresponding to exons 2 to 8 of *Cep63* expressed from pGEX-4T-1 (Amersham Biosciences) was used to generate a mouse monoclonal IgG<sub>1</sub> antibody (DCS 390) by standard hybridoma technology, which showed specificity for immunostaining, immunoblotting, and immunoprecipitation (Figs. 1B and C and 2A; Supplementary Figs. S2B, E, S3A, and S7). Other antibodies used were mouse mono-

clonals to  $\gamma$ -tubulin (TU-30; Exbio), Eg5 (BD Transduction Laboratories), Cdk1 (clone 17; Santa Cruz), centrin (20H5; provided by J.L. Salisbury), Cep170 (77-419; provided by E.A. Nigg), C-Nap1 (clone 42; BD Transduction Laboratories); GFP (B-2; Santa Cruz), phospho-Ser139 histone H2AX ( $\gamma$ -H2AX; JBW301; Upstate), rabbit polyclonals to  $\gamma$ -tubulin (T 5192; Sigma), actin (I-19 or C4; Santa Cruz), GFP (FL; Santa Cruz), pericentrin (ab4448; Abcam), phospho-Ser10 histone H3 (Upstate #06-570), and a rabbit monoclonal to Myc-tag (71D10; Cell Signaling).

### Immunofluorescence, metaphase spreads, and live cell imaging

Standard protocols were applied for immunofluorescence of cells grown on coverslips or collected by cytocentrifugation (Shandon Cytospin 3) and for metaphase spreads. Fluorescence microscopy was done using Zeiss Axiovert 200 M, LSM 510 and LSM 710 (Zeiss Application Center) microscopes equipped with A-Plan 10 $\times$ /0.25, Plan-Neofluar 40 $\times$ /1.3, Plan-Neofluar 100 $\times$ /1.3, and Plan-Apochromat 63 $\times$ /1.4 objectives and Zeiss AxioVision and ZEN 2008 software. Time-lapse video microscopy of cells grown on  $\mu$ -Dishes (Ibidi #81166 or #80136) was carried out at 37°C in a humidified atmosphere containing 5% CO<sub>2</sub>, using a Zeiss Cell Observer (DKFZ Light Microscopy Facility) or the Nikon BioStation IM system (Nikon Imaging Centre).

### Microinjection

Microinjection of siRNAs (final concentration 25–80  $\mu$ M/L) and rhodamine B isothiocyanate-dextran (average mol wt 20,000; Sigma-Aldrich; final concentration 0.5%, w/v) was conducted on an Olympus IX70 microscope with a semiautomatic Eppendorf microinjection system (Microinjector 5242 and Micromanipulator 5171). All experiments included *Cep63*-siRNA and control *luciferase* siRNA-injected cells in 2 distinct areas on the same dish featuring a grid pattern to relocate injected cells. All injected cells were individually traced to determine cell fates. Cell sizes were measured after manual delineation of cell boundaries using AxioVision 4.7.2 software (Zeiss).

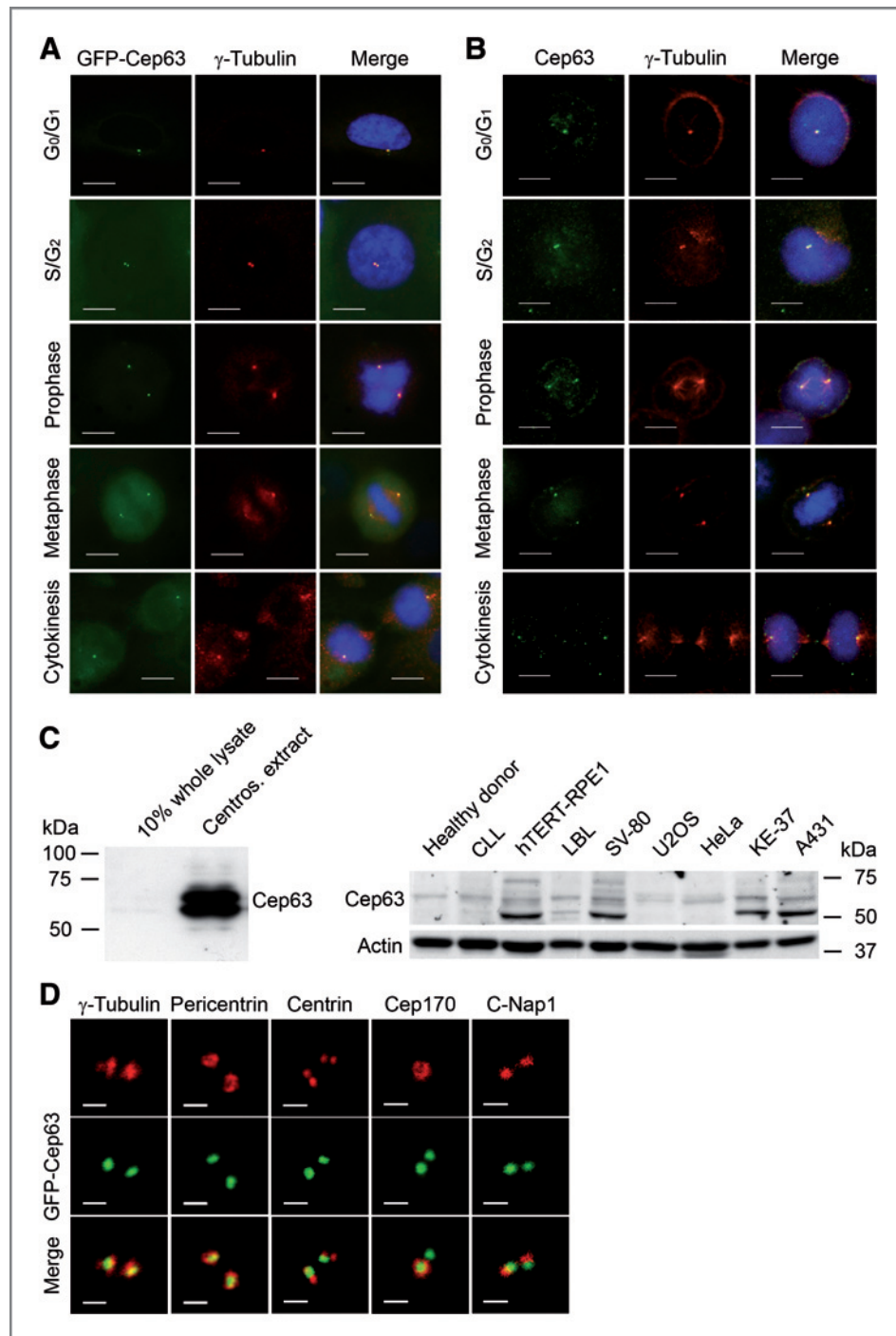
### Quantification of centrosomal proteins

Using a Zeiss LSM 710 laser scanning microscope (Zeiss Application Center), 3-dimensional confocal data sets from a defined volume containing the centrosome (verified by  $\gamma$ -tubulin staining) were collected under standardized settings. The volume of signals exceeding a standardized threshold was calculated using AxioVision 4.7.2 software (Zeiss).

### GST pulldown assay, immunoprecipitation, centrosome extraction, and immunoblotting

The cDNA of *Cdk1* (transcript variant 3, encoding isoform 1) cloned into pcDNA3.1/Myc-His (Invitrogen) was subjected to *in vitro* transcription/translation with <sup>35</sup>S-labeling by using the TNT Quick Coupled Transcription/Translation System (Promega) following the manufacturer's instructions. *In vitro* GST pulldown assays using a GST-fusion peptide corresponding to

**Figure 1.** Cep63 is a constitutive centrosomal protein. **A**, in U2OS cells conditionally expressing GFP-Cep63, transgene expression was induced for 72 hours. Cells were immunostained for  $\gamma$ -tubulin (red). DNA was counterstained with DAPI (blue). Scale bars, 10  $\mu$ m. **B**, exponentially growing U2OS cells were immunostained for Cep63 (green) and  $\gamma$ -tubulin (red). DNA was counterstained with DAPI (blue). Scale bars, 10  $\mu$ m. **C**, immunoblots for Cep63 using a centrosome extract made from KE-37 cells compared with 20  $\mu$ g of whole lysate (10% of the input) from the same cell line (left) and 150  $\mu$ g protein extract per lane from different cell lines, EBV-transformed lymphoblastoid cells (LBL), and peripheral blood mononuclear cells from a healthy donor and a patient with CLL (right). Actin was used as a loading control. **D**, in U2OS cells conditionally expressing GFP-Cep63, transgene expression was induced for 72 hours. Cells were immunostained for the indicated proteins (red). Centrosomes were focused by laser scanning microscopy. Scale bars, 1  $\mu$ m.



full-length *Cep63* (transcript variant 3) expressed from pGEX-4T-1 (Amersham Biosciences), immunoprecipitation using a 1:1 mixture of protein A-agarose and protein G-agarose (Roche), centrosome extraction from KE-37 cells, and immunoblotting were carried out following established protocols (28, 29). If not indicated otherwise, control fractions for immunoprecipitates (bound) were 5% of the input protein

extract and 5% of the supernatant from the immunoprecipitation reaction (unbound).

#### Flow cytometry

Standard protocols were applied for staining of cells with propidium iodide (Molecular Probes) with or without staining for phospho-Ser10-histone H3. Cells were subjected to flow

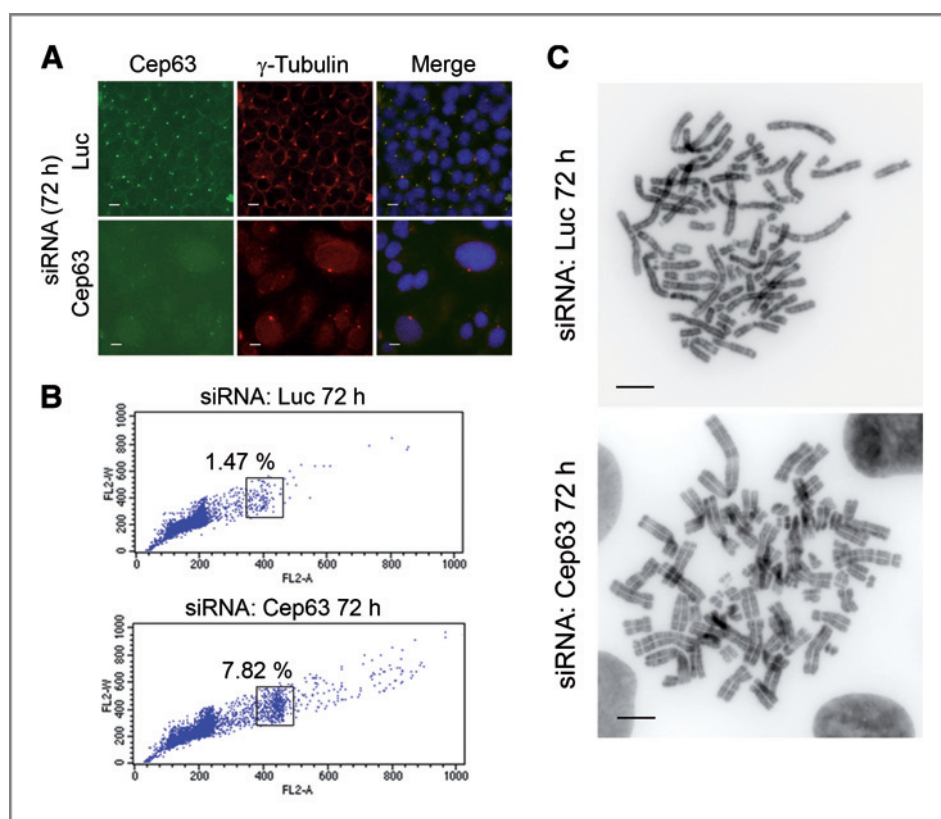


Figure 2. Cep63 downregulation induces polyploidization. A, U2OS cells were transfected with siRNA to *luciferase* (Luc) or *Cep63*, respectively, harvested after 72 hours, and immunostained for Cep63 (green) and  $\gamma$ -tubulin (red). DNA was counterstained with DAPI (blue). Scale bars, 10  $\mu$ m. B, U2OS cells were transfected with siRNA to *luciferase* (Luc) or *Cep63*, respectively, for 72 hours. After propidium iodide staining, the DNA content was measured by flow cytometry. C, metaphase spreads of U2OS cells were prepared 72 hours after transfection with siRNA to *luciferase* (Luc) or *Cep63*, respectively. Scale bars, 20  $\mu$ m.

cytometry by using a FACScan (BD Biosciences) flow cytometer.

#### Expression analysis of neuroblastoma samples

Cep63 mRNA expression in primary neuroblastomas was analyzed using oligo microarray as described (30, 31).

#### DNA DSB analysis

Twenty-four hours after induction of GFP-Cep63 expression, cells were synchronized by thymidine (3 mmol/L, 24 hours) and released into medium containing 2-deoxycytidine (24  $\mu$ mol/L) and, where indicated, aphidicolin (0.4  $\mu$ mol/L). When cells started entering mitosis, colcemide was added (1  $\mu$ g/mL). Eight hours later, metaphase spreads were prepared as described (32). Following  $\gamma$ -H2AX staining and image acquisition under standardized settings by using an Olympus BX50 fluorescent microscope equipped with a Cool Snap HQ2 digital camera (Photometrix),  $\gamma$ -H2AX foci in metaphases were analyzed as described (Supplementary Fig. S8; ref. 33).

#### Statistical analysis

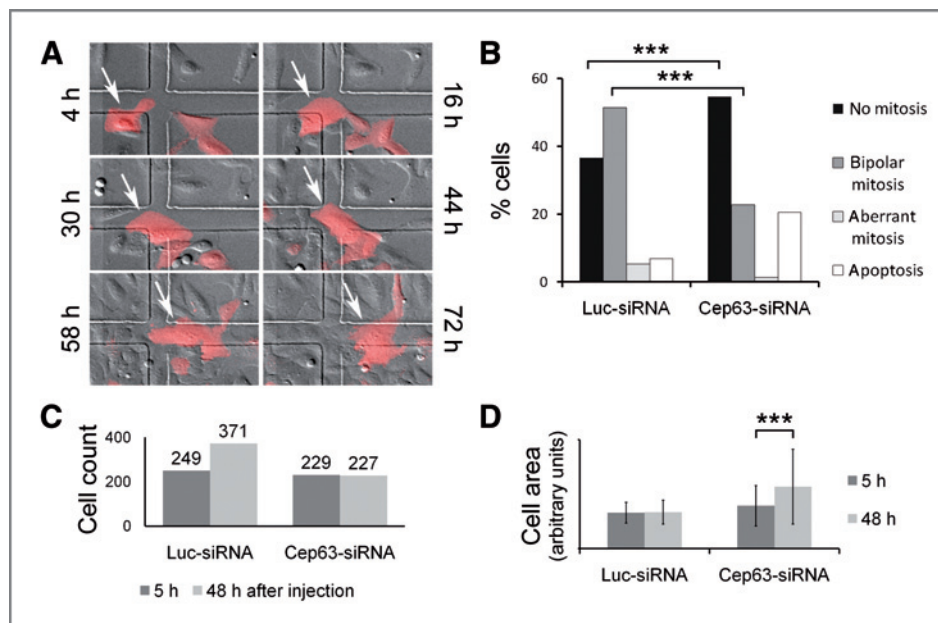
If not indicated otherwise, results are given as mean  $\pm$  SD. Significances were determined using the heteroscedastic, 2-tailed Student *t* test or the  $\chi^2$  test. To identify a model describing the relationship between survival and Cep63 expression, the functional form of the relationship was tested by maximally selected log-rank statistics (30).

## Results

### Cep63 is a constitutive centrosomal protein

Consistent with the initial report (25), transiently expressed GFP-Cep63 almost exclusively localized to centrosomes in several cell lines, with no differences among isoforms (Supplementary Figs. S1 and S2A). Since quantitative RT-PCR revealed that among the 4 known transcript variants variant 3 was most abundant (Supplementary Fig. S1B), we used this variant to generate U2OS cells stably expressing GFP-Cep63 in a tetracycline-dependent manner and found GFP-Cep63 virtually exclusively localized to centrosomes in all cell-cycle phases (Fig. 1A). Immunostaining with a mouse monoclonal antibody revealed that endogenous Cep63 almost exclusively localized to centrosomes throughout the cell cycle in all cell lines tested (Fig. 1B; Supplementary Fig. S2B and C). This pattern remained unaltered upon microtubule disruption (Supplementary Fig. S2D), confirming Cep63 to be a constitutive centrosomal protein. The centrosomal localization was verified by examining centrosome extracts, and in a panel of human normal, immortalized, and tumor cell lines, endogenous Cep63 was always present, with 2 prominent bands corresponding to isoforms 2 (63 kDa) and 3 (58 kDa) on immunoblots (Fig. 1C). In immunofluorescence analyses, the number of Cep63 signals regularly matched the number of  $\gamma$ -tubulin or pericentrin signals, respectively (Fig. 1A, B, and D). Detailed colocalization analysis by laser scanning

**Figure 3.** Live cell imaging of Cep63-depleted cells. \*\*\*, all indicated differences are highly significant ( $P < 0.001$ ). A, U2OS cells were injected with Cep63-siRNA and rhodamine (red) and followed by time-lapse video microscopy from 4 to 72 hours after injection (Supplementary Video S1). B to D, a total of 229 U2OS cells were injected with 25  $\mu\text{mol/L}$  Cep63-siRNA and rhodamine-dextran, whereas 249 control cells on the same dish were injected with 25  $\mu\text{mol/L}$  *luciferase*-siRNA and rhodamine-dextran. Individual cell fates within the period from 5 to 48 hours after injection (B), cell counts (C), and cell areas (D) were assessed.



microscopy revealed that GFP-Cep63 mostly localized within the region positive for  $\gamma$ -tubulin and pericentrin while showing a partial overlap with C-Nap1 but only little overlap with centrin and Cep170 (Fig. 1D), indicating that Cep63 is a centrosomal but probably not core centriolar protein.

### Cep63 downregulation induces polyploidization due to mitotic skipping

Using a siRNA targeting all known isoforms of *Cep63* (Fig. 2A; Supplementary Figs. S2E and S3A and B), we depleted Cep63 in U2OS cells and found a striking accumulation of giant cells (Fig. 2A; Supplementary Fig. S3C). By 72 hours posttransfection, flow cytometry revealed a significant increase of cells with more than 4N DNA from  $3.5\% \pm 0.4\%$  in *luciferase*-siRNA-treated cells to  $11.0\% \pm 2.0\%$  after treatment with *Cep63*-siRNA ( $P = 0.019$ ; mean  $\pm$  SD of 3 independent experiments). When only cells with 8N DNA were counted, this increase was likewise significant ( $P = 0.021$ ) with  $1.6\% \pm 0.3\%$  of cells after *luciferase*-siRNA but  $6.3\% \pm 1.3\%$  of cells after *Cep63*-siRNA harboring 8N DNA (Fig. 2B). This phenotype was confirmed by using an alternative siRNA against *Cep63* (Supplementary Fig. S3D and E; Supplementary Table S1). Polyploidization was further confirmed by a significant increase ( $P = 0.010$ ) of metaphases harboring diplochromosomes to  $4.0\% \pm 1.0\%$  (mean  $\pm$  SD of 3 times 100 metaphase spreads) 72 hours after treatment with *Cep63*-siRNA, a 12-fold increase compared with  $0.3\% \pm 0.6\%$  of metaphases after control *luciferase*-siRNA (Fig. 2C).

To differentiate between skipping of mitosis, failed mitosis, or cell fusion underlying polyploidization, we conducted time-lapse video microscopy after direct microinjection of siRNA to *Cep63* into U2OS cells. In repeated sessions using a variety of conditions and compassing up to

72 hours postmicroinjection, we observed neither cell fusions nor increased rates of aberrant or failed mitoses in Cep63-depleted cells compared with cells injected with *luciferase*-siRNA. Instead, the majority of mitoses seemed normal and a subset of *Cep63* siRNA-injected cells displayed enlargement without intervening mitoses consistent with mitotic skipping (Fig. 3A; Supplementary Video S1). Quantification in 478 injected cells revealed a highly significant decrease of the mitotic rate because of Cep63 depletion ( $P = 4.44\text{E-}13$ ; Fig. 3B). Instead, the proportion of cells remaining in interphase was highly significantly elevated compared with cells injected with *luciferase*-siRNA ( $P = 1.82\text{E-}06$ ; Fig. 3B). Whereas proliferation resulted in an increased amount of control cells, the number of Cep63-depleted cells remained stable during the experiments (Fig. 3C). Consistent with mitotic skipping leading to endopolyploidization, Cep63-depleted cells remaining in interphase during observation showed a highly significant increase in cell size ( $P = 1.19\text{E-}06$ ) whereas *luciferase*-siRNA-injected controls remaining in interphase displayed a stable size (Fig. 3D). Notably, 22.7% of all *Cep63*-siRNA-injected cells compared with 2.4% of *luciferase*-siRNA-injected cells ( $P = 1.12\text{E-}11$ ) showed a more than 1.5-fold size increase while remaining in interphase, indicating that after direct microinjection of *Cep63*-siRNA, the proportion of cells becoming polyploid is substantially higher than after conventional siRNA transfection.

Mitotic skipping was further confirmed by live imaging of microinjected cells released from a thymidine block revealing that 203 of 320 cells injected with *luciferase*-siRNA (63%), but only 57 of 265 cells injected with *Cep63*-siRNA (22%), passed through mitosis as expected between 6 and 24 hours after release ( $P = 3.02\text{E-}24$ ). In addition, *Cep63*-siRNA-injected U2OS cells stably expressing GFP- $\alpha$ -tubulin allowing

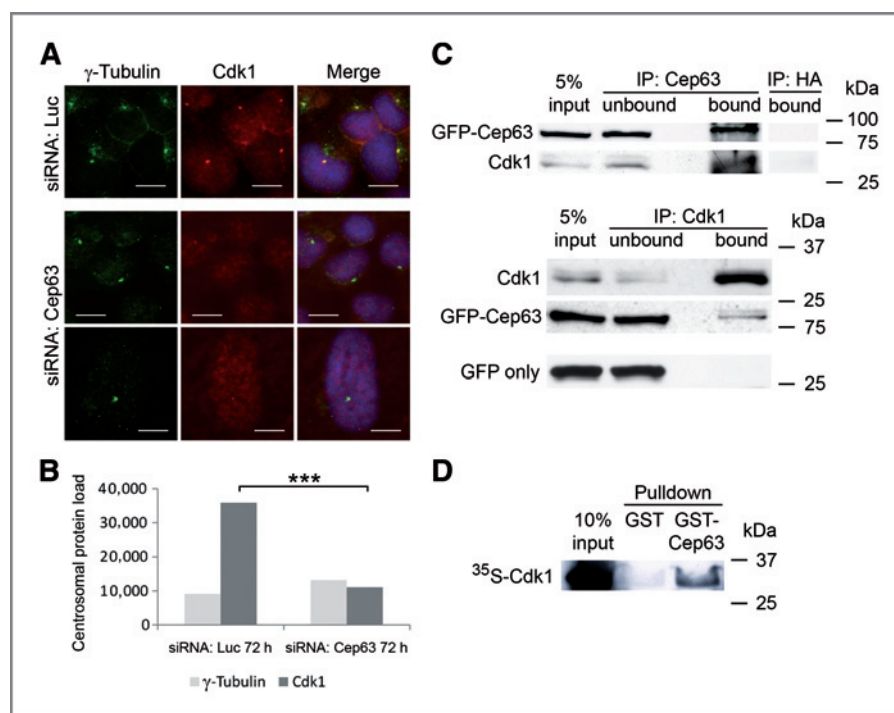


**Figure 4.** Cep63 recruits Cdk1 to the centrosome. **A**, U2OS cells were transfected with siRNA to *luciferase* (Luc) or *Cep63*, respectively, fixed after 72 hours, and immunostained for  $\gamma$ -tubulin (green) and Cdk1 (red). DNA was counterstained with DAPI (blue). Scale bars, 10  $\mu$ m. **B**, in U2OS cells processed as in **A**, the centrosomal load of the respective protein was quantified in 50 cells per data bar. \*\*\*, this difference is highly significant ( $P = 0.00028$ ). **C**, immunoprecipitation (IP) from 2 mg protein extract per lane of U2OS cells induced to express GFP-Cep63 or U2OS cells transfected with empty pEGFP-C1 plasmid was conducted with antibodies to the indicated protein, followed by immunoblotting using antibodies to Cep63 (first row), Cdk1, or GFP (fourth and fifth rows), respectively. **D**, GST pull-down assays with *in vitro* translated  $^{35}$ S-Cdk1 and GST or GST-Cep63, respectively. As input control, 10% of the amount of  $^{35}$ S-Cdk1 used for each pull-down was loaded.

visualization of mitotic spindles showed no evidence of mitotic aberrations during live imaging (Supplementary Fig. S3F), and quantification on fixed cells revealed a proportion of  $89.8\% \pm 6.1\%$  (mean  $\pm$  SD of 4 times 100 mitoses) normal bipolar mitoses in U2OS cells 72 hours after transfection with *Cep63*-siRNA as compared with  $96.0\% \pm 1.4\%$  after control siRNA ( $P = 0.13$ ). Overall, several complementary approaches show that *Cep63* depletion leads to inhibition of mitotic entry, with subsequent polyploidization due to endoreplication in a subset of cells, and without inducing significant mitotic aberrations.

#### Cep63 recruits Cdk1 to the centrosome

Mitosis is initiated by activation of centrosomal cyclin B1-Cdk1 (19, 21). Lack of Cdk1 activation is associated with skipping of mitosis and endoreplication (23, 34). Hence, we asked whether mitotic skipping in *Cep63*-depleted cells reflects lack of centrosomal Cdk1. Immunofluorescence revealed a pronounced decrease of the centrosomal Cdk1 load after *Cep63* downregulation in U2OS cells (Fig. 4A and B). Giant cells observed after *Cep63*-siRNA showed notably low levels of centrosomal Cdk1, consistent with the model that polyploidization after *Cep63* depletion results from a lack of centrosomal Cdk1 (Fig. 4A). A direct interaction between *Cep63* and Cdk1 was verified by both coimmunoprecipitation and an *in vitro* GST pull-down assay using GST-tagged full-length *Cep63*

(Fig. 4C and D). Interestingly, coimmunoprecipitation failed to reveal any evidence for an interaction between *Cep63* and cyclin B, A, or E (Supplementary Fig. S4A). Finally, siRNA-mediated depletion of Cdk1 led to a polyploidization phenotype virtually identical to that observed after *Cep63* depletion (Supplementary Fig. S4B). We conclude that initiation of mitosis requires centrosomal recruitment of Cdk1 by *Cep63*.

#### Cep63 overexpression induces *de novo* centrosome amplification in interphase

We observed increased numbers of cells with supernumerary centrosomes both after transient overexpression of GFP-Cep63 (Supplementary Fig. S5A) and in U2OS cells conditionally expressing GFP-Cep63, where centrosome amplification was detectable by 24 to 48 hours and reached a maximum about 72 hours after GFP-Cep63 induction, when a steady state was reached, presumably due to elimination of cells with amplified centrosomes (Fig. 5A and B). To rule out secondary centrosome amplification due to polyploidization, we induced GFP-Cep63 for up to 2 weeks, but no evidence for polyploidization was found (Supplementary Fig. S5B). Time-lapse video microscopy revealed that *Cep63* overexpression was associated with centrosome amplification occurring during interphase (Fig. 5C; Supplementary Video S2). Regularly, gradual accumulation of supernumerary centrosomes in a single interphase was

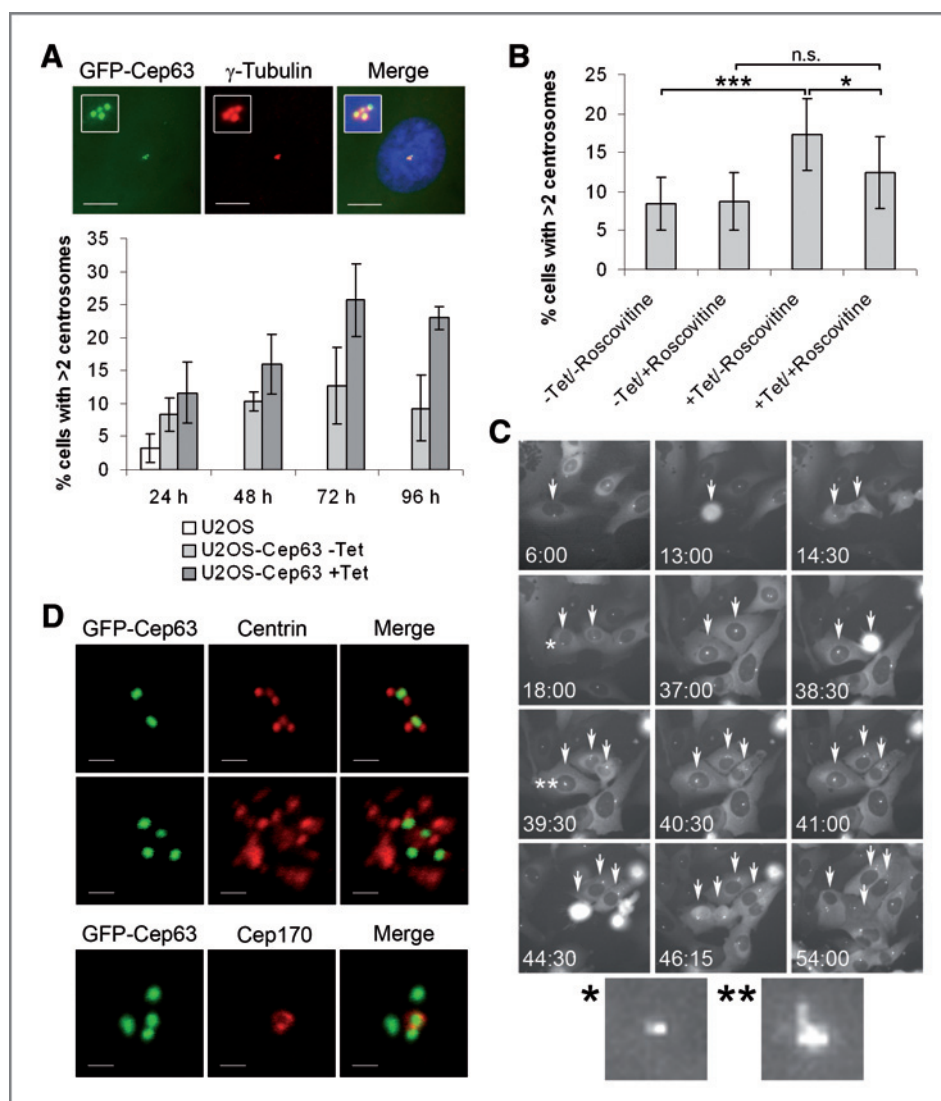


**Figure 5.** Cep63 overexpression induces *de novo* centrosome amplification in interphase. All experiments were carried out with U2OS cells conditionally expressing GFP-Cep63. Centrosomes were identified and counted by  $\gamma$ -tubulin immunostaining. **A**, cells were induced to express GFP-Cep63 for the indicated times (dark gray bars) or were left untreated and harvested simultaneously (light gray bars). Parental U2OS cells were grown for 24 hours (white bar). At least 3 times, 100 cells per data bar were evaluated. Top, a representative cell where GFP-Cep63 expression was induced for 72 hours immunostained for  $\gamma$ -tubulin (red). DNA was counterstained with DAPI (blue). Scale bars, 10  $\mu$ m. Insets show higher magnifications of centrosomes. **B**, where indicated, cells were induced to express GFP-Cep63 for 72 hours, with or without simultaneous addition of roscovitine to a final concentration of 1  $\mu$ g/mL. Ten times 100 cells per data bar were evaluated. \*\*\*, this difference is highly significant ( $P = 0.00012$ ). \*, this difference is significant ( $P = 0.026$ ). n.s., this difference is not significant ( $P = 0.071$ ). **C**, following induction of GFP-Cep63 expression for the indicated times (hours: minutes), GFP fluorescence was monitored by time-lapse microscopy (Supplementary Video S2). A representative example is marked by arrows. Originating from one mother cell, both daughter cells show *de novo* centrosome amplification in interphase followed by mitoses, with supernumerary centrosomes in their daughter cells as well. A centrosome before (\*) and after (\*\*) amplification, as marked in the main panel, is shown enlarged below. It should be noted that the number of GFP-Cep63 signals can be used as a marker of the centrosome number (Fig. 1D). **D**, confocal images of centrosomes in U2OS cells conditionally expressing GFP-Cep63 immunostained for centrin (red; top and middle) or Cep170 (red; bottom). Transgene expression was induced for 72 hours. Scale bars, 1  $\mu$ m.

followed by a normal bipolar mitosis, which is consistent with centrosomal clustering preventing spindle multipolarity (15, 16, 35). The daughter cells resulting from these mitoses often harbored amplified centrosomes as well (Fig. 5C; Supplementary Video S2).

During Cep63 overexpression, the number of centrin signals often exceeded twice the number of GFP-Cep63 signals, indicating that centriole overduplication preceded maturation

with recruitment of Cep63 to overduplicated centrosomes (Fig. 5D). Amplified centrosomes were associated with only one signal of Cep170, a marker of mature centrioles (36), further confirming *de novo* centrosome amplification during interphase (Fig. 5D).

As Cdk inhibition by roscovitine suppressed centrosome amplification upon induction of GFP-Cep63 (Fig. 5B), we asked whether this phenotype was mediated by Cdk1 or Cdk2. Since

Cdk1 overexpression induced centrosome amplification (Supplementary Fig. S5C), centrosomal overrecruitment of Cdk1 likely plays a role in Cep63-induced centrosome amplification. On the other hand, coimmunoprecipitation indicated that Cep63 also interacts with Cdk2, although weaker than with

Cdk1 (Supplementary Fig. S5D). Hence, we cannot exclude that Cdk2 contributes to this phenotype as well. However, we were unable to confirm a direct interaction with Cdk2 in an *in vitro* GST pull-down assay using GST-Cep63.

### The N-terminus of Cep63 is necessary and sufficient for its centrosomal localization and centrosome amplification

Using GFP-tagged deletion constructs of Cep63, we found that the N-terminus comprising amino acids 1 to 290 was necessary and sufficient to promote both the centrosomal localization of Cep63 and centrosome amplification (Supplementary Fig. S6). Our data indicate that Cep63-induced centrosome amplification depends on the centrosomal localization of Cep63 and that the common N-terminus of all 4 known isoforms of Cep63 consisting of amino acids 1 to 309 (Supplementary Fig. S1) harbors the minimal functional sequence of Cep63.

### Cep63 overexpression is associated with aggressive malignancies and promotes chromosomal breakage

Since Cdk deregulation and centrosome amplification are likely oncogenic mechanisms, we speculated that Cep63 might be overexpressed in malignant cells. Indeed, analysis of mRNA expression data of 244 human neuroblastomas revealed a correlation between high *Cep63* expression levels and advanced stage (stage 4) of the disease (Fig. 6A). Moreover, high *Cep63* levels were associated with *MYCN* oncogene amplification and poor survival (Fig. 6A and B).

In addition to Cdk-dependent centrosome amplification, Cep63-triggered Cdk deregulation might also impair the DNA damage response and lead to persistence of unrepaired replication-associated defects in the form of DNA DSBs in mitotic cells (37–39). We therefore evaluated whether DSB signaling and frequency might be enhanced in Cep63-overexpressing cells exposed to replication stress. Indeed, treatment with aphidicolin, which induces DNA DSBs by inhibiting DNA polymerases (40), led to an increase in the amount of  $\gamma$ -H2AX, a DSB marker, in metaphases of Cep63-overexpressing as compared with control cells (Fig. 6C). We conclude that Cep63 overexpression is associated with aggressive malignancies, wherein it might contribute to the aggressive behavior of these tumors by impairing the DNA damage response and propagation of unrepaired chromosomal breaks.

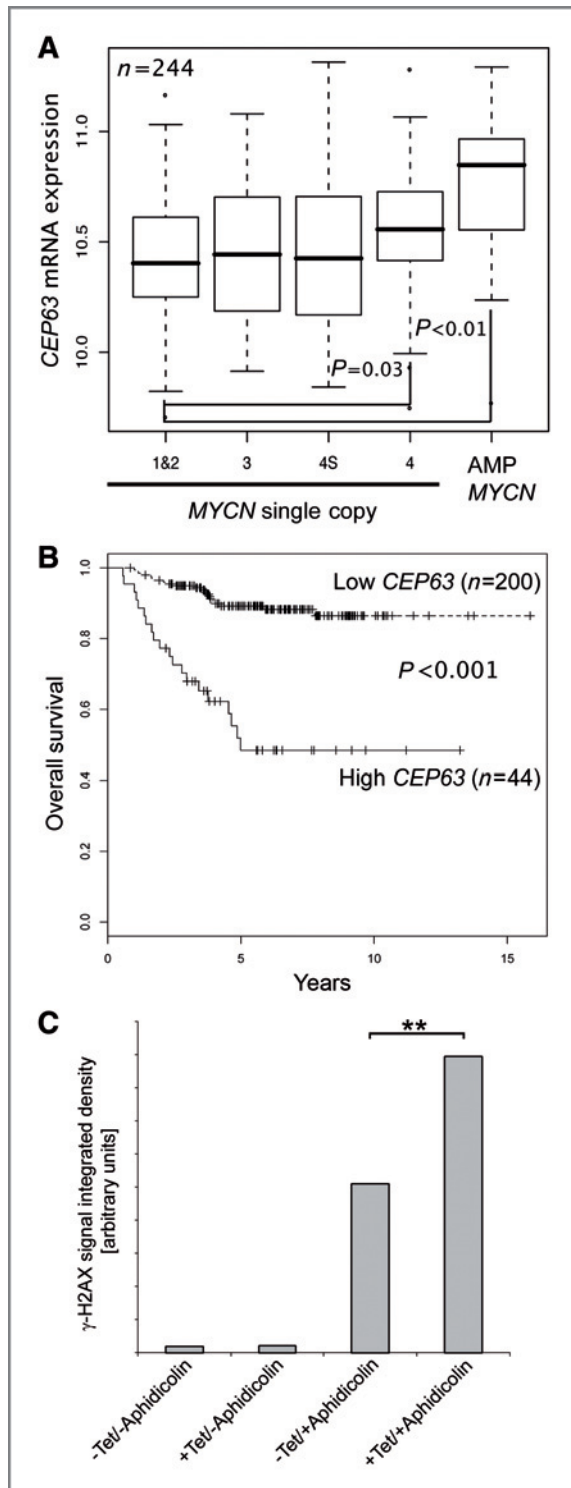


**Figure 6.** Cep63 overexpression is associated with aggressive malignancies and DNA DSBs. **A**, 244 neuroblastoma patients were classified according to the International Neuroblastoma Staging System (49), except for cases with *MYCN* amplification, which were separately evaluated and, together with stage 4, represent the poorest prognosis group. Relative expression levels of *Cep63*-mRNA are given as box plots where the boundaries represent the 25th and 75th percentiles, while the median is indicated by a horizontal line within the box. **B**, Kaplan-Meier plots of overall survival of 244 neuroblastoma patients classified according to their *Cep63*-mRNA expression level. The optimal cutoff level (10.83091) between high and low *Cep63* expression was determined by log-rank statistics. **C**, as indicated, GFP-Cep63 expression was induced with or without addition of aphidicolin. The  $\gamma$ -H2AX signal integrated densities were quantified by immunofluorescence of at least 100 metaphase spreads per data bar. \*\*, this difference is significant ( $P = 0.0023$ ).

## Discussion

In this study, we show that human Cep63 is a constitutive centrosomal protein exhibiting a virtually exclusive centrosomal localization throughout the cell-cycle independent of the presence of microtubules. We show that Cep63 directly interacts with and thereby recruits Cdk1 to centrosomes as a prerequisite for mitotic entry. Moreover, we show that Cep63 overexpression leads to *de novo* centrosome amplification and a link between Cep63 overexpression to aggressive malignancies and an impaired DNA damage response has been established.

Cdk1 localizes to centrosomes throughout the cell cycle where initial activation of the cyclin B1–Cdk1 complex and subsequent initiation of mitosis occurs (19, 21, 41). Cdk2 has been described to localize to centrosomes as well (42). Cyclins A, B1, and E are recruited to centrosomes independently of Cdks via their centrosomal localization signals, the centrosomal binding partners of which are currently unknown (24, 43). Consequentially, it is believed but unproven that Cdks are indirectly targeted to centrosomes via their partner cyclins. Our data for the first time provide evidence that Cdk1 is directly recruited to centrosomes via interaction with Cep63. Support for this contention is manifold: First, we show that Cep63 and Cdk1 directly interact with each other whereas no interaction between cyclins and Cep63 was found. Second, knockdown of Cep63 by siRNA led to a specific depletion of Cdk1 from centrosomes and phenocopied direct knockdown of Cdk1 with mitotic skipping and polyploidization.

In a study on *Xenopus* mitotic egg extracts, Cep63 downregulation induced aberrant mitoses, which was explained by a lack of centrosomal Cep63 causing inhibition of spindle assembly during mitosis (26). In mammalian cells, we now describe that Cep63 depletion suppressed mitotic entry altogether, which led to mitotic skipping in a subset of cells. This phenotype was not associated with abnormal mitoses since in cells where Cep63 was efficiently downregulated, G<sub>2</sub> phase was directly followed by endoreplication. However, analogous to the situation in *Xenopus* mitotic egg extracts, depletion of Cep63 prevented successful cell division in mammalian cells.

As further evidence for a functionally relevant interaction between Cep63 and Cdk1, we show that Cep63 overexpression leads to *de novo* centrosome amplification during interphase. We have shown that centrosome amplification can be induced by Cdk1 overexpression and Cep63-induced centrosome amplification can be suppressed by roscovitine, and published evidence suggests that Cdk2 is dispensable for centrosome duplication and amplification (14, 44), which together support the notion that overrecruited Cdk1 contributes to Cep63-induced centrosome amplification. A weak interaction between Cep63 and Cdk2, as indicated by our coimmunoprecipitation data, might additionally contribute to centrosome amplification when Cep63 is overexpressed also because Cdk1 and Cdk2 are closely related in structure (45). We conclude that the interaction of Cdk1 with Cep63 sufficiently explains all observed phenotypes whereas the

potential functional link between Cep63 and Cdk2 remains speculative.

Finally, we show an association of Cep63 overexpression with aggressive behavior of human neuroblastomas and an impaired DNA damage response to replication stress, a condition shared by many oncogene-transformed cells and the majority of human neoplasms (37–39). The increased rate of DNA DSBs we observed in the presence of aphidicolin might be explained by elevated Cep63 causing Cdk hyperactivation and, consequently, an override of checkpoint mechanisms that normally guard against mitotic entry with unrepaired chromosomes. In broad terms, this phenotype resembles other types of Cdk deregulation such as Chk1 inhibition or overexpression of the oncogenic Cdc25A phosphatase (46, 47). An alternative mechanism about how overexpressed Cep63 contributes to malignant phenotypes may be centrosome amplification leading to chromosomal instability by promoting chromosome missegregation (17). Specifically relating to *MYC* oncogene, it has been shown that *MYCN* overexpression in neuroblastoma cells induces centrosome hyperamplification after induction of DNA DSBs (48).

In summary, our data identify Cep63 as a centrosomal recruitment factor for Cdk1 and may help to better understand both the centrosomal regulation of mitotic entry and the phenomenon of centrosome amplification, which is common in malignant cells, presumably underlying cancer-associated chromosomal instability (7, 17). In addition, Cep63-induced centrosome amplification might be part of the centrosome inactivation checkpoint, a proposed backup checkpoint mechanism promoting mitotic catastrophe (2, 7, 9–12). Moreover, we identify a link between Cep63, oncogenesis, and the DNA damage response in human cells, which extends and complements the established role of Cep63 in the regulation of centrosome-dependent spindle assembly after DNA DSBs in *Xenopus* (26).

## Disclosure of Potential Conflicts of Interest

No potential conflicts of interest were disclosed.

## Acknowledgments

We thank E.A. Nigg, J.L. Salisbury, L. Savelyeva, G. Stöcklin, and G. Pereira for reagents; B. Tews, A. Tibelius, F. Bestvater, M. Brom, U. Engel, S. Poppelreuther, P. Lichter, and A. Poustka for technical support; and M. Czeranski, S. Henemann, and B. Schreiter for excellent technical assistance. Support by the DKFZ Light Microscopy Facility, the Zeiss Application Center, and the Nikon Imaging Center is gratefully acknowledged.

## Grant Support

This work was supported by the Deutsche Krebshilfe (grant 108560), Danish National Research Foundation, the Czech Ministry of Education (MSM6198959216), the Czech Ministry of Health (NT/11065-5/2010), the Lundbeck Foundation (R13-A1287), the European Commission projects: EET pipeline (FP5, 037260), Biomedreg (CZ.1.05/2.1.00/01.0030), Infla-Care (FP7), and the Stiftung für Krebs- und Scharlachforschung Mannheim.

The costs of publication of this article were defrayed in part by the payment of page charges. This article must therefore be hereby marked *advertisement* in accordance with 18 U.S.C. Section 1734 solely to indicate this fact.

Received July 22, 2010; revised November 16, 2010; accepted January 10, 2011; published online March 15, 2011.

## References

1. Doxsey S. Re-evaluating centrosome function. *Nat Rev Mol Cell Biol* 2001;2:688–98.
2. Nigg EA. Centrosome aberrations: cause or consequence of cancer progression? *Nat Rev Cancer* 2002;2:815–25.
3. Meraldi P, Lukas J, Fry AM, Bartek J, Nigg EA. Centrosome duplication in mammalian somatic cells requires E2F and Cdk2-cyclin A. *Nat Cell Biol* 1999;1:88–93.
4. Hinchcliffe EH, Li C, Thompson EA, Maller JL, Sluder G. Requirement of Cdk2-cyclin E activity for repeated centrosome reproduction in *Xenopus* egg extracts. *Science* 1999;283:851–4.
5. Lacey KR, Jackson PK, Stearns T. Cyclin-dependent kinase control of centrosome duplication. *Proc Natl Acad Sci U S A* 1999;96:2817–22.
6. Matsumoto Y, Hayashi K, Nishida E. Cyclin-dependent kinase 2 (Cdk2) is required for centrosome duplication in mammalian cells. *Curr Biol* 1999;9:429–32.
7. Krämer A. Centrosome aberrations—hen or egg in cancer initiation and progression? *Leukemia* 2005;19:1142–4.
8. Löffler H, Lukas J, Bartek J, Krämer A. Structure meets function—centrosomes, genome maintenance and the DNA damage response. *Exp Cell Res* 2006;312:2633–40.
9. Takada S, Kelkar A, Theurkauf WE. *Drosophila* checkpoint kinase 2 couples centrosome function and spindle assembly to genomic integrity. *Cell* 2003;113:87–99.
10. Sibon OC, Kelkar A, Lemstra W, Theurkauf WE. DNA-replication/DNA-damage-dependent centrosome inactivation in *Drosophila* embryos. *Nat Cell Biol* 2000;2:90–5.
11. Dodson H, Bourke E, Jeffers LJ, Vagnarelli P, Sonoda E, Takeda S, et al. Centrosome amplification induced by DNA damage occurs during a prolonged G<sub>2</sub> phase and involves ATM. *EMBO J* 2004;23:3864–73.
12. Bourke E, Dodson H, Merdes A, Cuffe L, Zachos G, Walker M, et al. DNA damage induces Chk1-dependent centrosome amplification. *EMBO Rep* 2007;doi:10.1038/sj.embor.7400962.
13. Meraldi P, Honda R, Nigg EA. Aurora-A overexpression reveals tetraploidization as a major route to centrosome amplification in p53<sup>-/-</sup> cells. *EMBO J* 2002;21:483–92.
14. Duensing A, Liu Y, Tseng M, Malumbres M, Barbacid M, Duensing S. Cyclin-dependent kinase 2 is dispensable for normal centrosome duplication but required for oncogene-induced centrosome overduplication. *Oncogene* 2006;25:2943–9.
15. Quintyne NJ, Reing JE, Hoffelder DR, Gollin SM, Saunders WS. Spindle multipolarity is prevented by centrosomal clustering. *Science* 2005;307:127–9.
16. Leber B, Maier B, Fuchs F, Chi J, Riffel P, Anderhub S, et al. Proteins required for centrosome clustering in cancer cells. *Sci Transl Med* 2010;2:33ra88.
17. Ganem NJ, Godinho SA, Pellman D. A mechanism linking extra centrosomes to chromosomal instability. *Nature* 2009;460:278–82.
18. Doxsey S, Zimmerman W, Mikule K. Centrosome control of the cell cycle. *Trends Cell Biol* 2005;15:303–11.
19. De Souza CP, Ellem KA, Gabrielli BG. Centrosomal and cytoplasmic Cdc2/cyclin B1 activation precedes nuclear mitotic events. *Exp Cell Res* 2000;257:11–21.
20. Dutertre S, Cazales M, Quaranta M, Froment C, Trabut V, Dozier C, et al. Phosphorylation of CDC25B by Aurora-A at the centrosome contributes to the G<sub>2</sub>-M transition. *J Cell Sci* 2004;117:2523–31.
21. Jackman M, Lindon C, Nigg EA, Pines J. Active cyclin B1-Cdk1 first appears on centrosomes in prophase. *Nat Cell Biol* 2003;5:143–8.
22. Cazales M, Schmitt E, Montembault E, Dozier C, Prigent C, Ducommun B. CDC25B phosphorylation by Aurora-A occurs at the G<sub>2</sub>/M transition and is inhibited by DNA damage. *Cell Cycle* 2005;4:1233–8.
23. Krämer A, Mailand N, Lukas C, Syljuåsen RG, Wilkinson CJ, Nigg EA, et al. Centrosome-associated Chk1 prevents premature activation of cyclin-B-Cdk1 kinase. *Nat Cell Biol* 2004;6:884–91.
24. Matsumoto Y, Maller JL. A centrosomal localization signal in cyclin E required for Cdk2-independent S phase entry. *Science* 2004;306:885–8.
25. Andersen JS, Wilkinson CJ, Mayor T, Mortensen P, Nigg EA, Mann M. Proteomic characterization of the human centrosome by protein correlation profiling. *Nature* 2003;426:570–4.
26. Smith E, Dejsuphong D, Balestrini A, Hampel M, Lenz C, Takeda S, et al. An ATM- and ATR-dependent checkpoint inactivates spindle assembly by targeting CEP63. *Nat Cell Biol* 2009;11:278–85.
27. Schmitt M, Pawlita M. High-throughput detection and multiplex identification of cell contaminations. *Nucleic Acids Res* 2009;37:e119.
28. Lukas J, Bartek J. Immunoprecipitation of proteins under nondenaturing conditions. In: Celis JE, editor. *Cell Biology: A Laboratory Handbook*. San Diego: Academic Press; 1998. p. 489–94.
29. Moudjou M, Bornens M. Method of centrosome isolation from cultured animal cells. In: Celis JE, editor. *Cell Biology: A Laboratory Handbook*. San Diego: Academic Press; 1994. p. 595–604.
30. Westermann F, Henrich KO, Wei JS, Lutz W, Fischer M, König R, et al. High Skp2 expression characterizes high-risk neuroblastomas independent of MYCN status. *Clin Cancer Res* 2007;13:4695–703.
31. Westermann F, Muth D, Benner A, Bauer T, Henrich KO, Oberthuer A, et al. Distinct transcriptional MYCN/c-MYC activities are associated with spontaneous regression or malignant progression in neuroblastomas. *Genome biology* 2008;9:R150.
32. Nakamura A, Sedelnikova OA, Redon C, Pilch DR, Sinogeeva NI, Shroff R, et al. Techniques for gamma-H2AX detection. *Methods Enzymol* 2006;409:236–50.
33. Mistrik M, Oplustilova L, Lukas J, Bartek J. Low-dose DNA damage and replication stress responses quantified by optimized automated single-cell image analysis. *Cell Cycle* 2009;8:2592–9.
34. Itzhaki JE, Gilbert CS, Porter AC. Construction by gene targeting in human cells of a "conditional" CDC2 mutant that rereplicates its DNA. *Nat Genet* 1997;15:258–65.
35. Rebacz B, Larsen TO, Clausen MH, Rønne MH, Löffler H, Ho AD, et al. Identification of griseofulvin as an inhibitor of centrosomal clustering in a phenotype-based screen. *Cancer Res* 2007;67:6342–50.
36. Guarguaglini G, Duncan PI, Stierhof YD, Holmstrom T, Duensing S, Nigg EA. The forkhead-associated domain protein Cep170 interacts with Polo-like kinase 1 and serves as a marker for mature centrosomes. *Mol Biol Cell* 2005;16:1095–107.
37. Halazonetis TD, Gorgoulis VG, Bartek J. An oncogene-induced DNA damage model for cancer development. *Science* 2008;319:1352–5.
38. El Achkar E, Gerbault-Seureau M, Muleris M, Dutrillaux B, Debatisse M. Premature condensation induces breaks at the interface of early and late replicating chromosome bands bearing common fragile sites. *Proc Natl Acad Sci U S A* 2005;102:18069–74.
39. Freudenreich CH. Chromosome fragility: molecular mechanisms and cellular consequences. *Front Biosci* 2007;12:4911–24.
40. Schwartz M, Zlotorynski E, Goldberg M, Ozeri E, Rahat A, le Sage C, et al. Homologous recombination and nonhomologous end-joining repair pathways regulate fragile site stability. *Genes Dev* 2005;19:2715–26.
41. Bailly E, Doree M, Nurse P, Bornens M. p34cdc2 is located in both nucleus and cytoplasm; part is centrosomally associated at G<sub>2</sub>/M and enters vesicles at anaphase. *EMBO J* 1989;8:3985–95.
42. De Boer L, Oakes V, Beamish H, Giles N, Stevens F, Somodevilla-Torres M, et al. Cyclin A/cdk2 coordinates centrosomal and nuclear mitotic events. *Oncogene* 2008;27:4261–8.
43. Bentley AM, Normand G, Hoyt J, King RW. Distinct sequence elements of cyclin B1 promote localization to chromatin, centrosomes, and kinetochores during mitosis. *Mol Biol Cell* 2007;18:4847–58.
44. Bourke E, Brown JA, Takeda S, Hochegger H, Morrison CG. DNA damage induces Chk1-dependent threonine-160 phosphorylation and activation of Cdk2. *Oncogene*; 29:616–24.
45. Malumbres M, Barbacid M. Mammalian cyclin-dependent kinases. *Trends Biochem Sci* 2005;30:630–41.

46. Syljuäsen RG, Sørensen CS, Hansen LT, Fugger K, Lundin C, Johansson F, et al. Inhibition of human Chk1 causes increased initiation of DNA replication, phosphorylation of ATR targets, and DNA breakage. *Mol Cell Biol* 2005;25:3553–62.
47. Bartkova J, Hořejší Z, Koed K, Tort F, Zieger K, Guldborg P, et al. DNA damage response as a candidate anti-cancer barrier in early human tumorigenesis. *Nature* 2005;434:864–70.
48. Sugihara E, Kanai M, Matsui A, Onodera M, Schwab M, Miwa M. Enhanced expression of MYCN leads to centrosome hyperamplification after DNA damage in neuroblastoma cells. *Oncogene* 2004;23:1005–9.
49. Brodeur GM, Pritchard J, Berthold F, Carlsen NL, Castel V, Castellberry RP, et al. Revisions of the international criteria for neuroblastoma diagnosis, staging, and response to treatment. *J Clin Oncol* 1993;11:1466–77.

# Cancer Research

The Journal of Cancer Research (1916–1930) | The American Journal of Cancer (1931–1940)

## Cep63 Recruits Cdk1 to the Centrosome: Implications for Regulation of Mitotic Entry, Centrosome Amplification, and Genome Maintenance

Harald Löffler, Anne Fechter, Marc Matuszewska, et al.

*Cancer Res* 2011;71:2129-2139.

**Updated version** Access the most recent version of this article at:  
<http://cancerres.aacrjournals.org/content/71/6/2129>

**Supplementary Material** Access the most recent supplemental material at:  
<http://cancerres.aacrjournals.org/content/suppl/2011/03/09/71.6.2129.DC1>

**Cited articles** This article cites 44 articles, 16 of which you can access for free at:  
<http://cancerres.aacrjournals.org/content/71/6/2129.full.html#ref-list-1>

**Citing articles** This article has been cited by 8 HighWire-hosted articles. Access the articles at:  
</content/71/6/2129.full.html#related-urls>

**E-mail alerts** [Sign up to receive free email-alerts](#) related to this article or journal.

**Reprints and Subscriptions** To order reprints of this article or to subscribe to the journal, contact the AACR Publications Department at [pubs@aacr.org](mailto:pubs@aacr.org).

**Permissions** To request permission to re-use all or part of this article, contact the AACR Publications Department at [permissions@aacr.org](mailto:permissions@aacr.org).